Geostrophic Response of the Yellow Sea to Cyclone Passage

IM SANG OH AND MARINA M. SUBBOTINA*

Department of Oceanography, Seoul National University, Seoul 151-742, Korea

A barotropic non-linear numerical model is used to study the response of the Yellow Sea to winter cyclone passage. Cyclones normally come from the outside of the western boundary, China, and pass the region eastward. The cyclone parameters used for the present study are the following: the intensity, i.e., the maximum wind speed of the cyclone; the effective radius corresponding to this maximum; and the translation speed. The equations of motion are integrated over the depth which is supposed to be a constant. The Gaussian function is used to define the stream function of the wind.

The following results have been found. A northward current is generated by the frontal part of the cyclone near the western boundary. After the cyclone leaves the sea area, a southward current is generated by the rear part of the cyclone. After that, a northward current is generated once again due to the westward propagating Rossby waves. The response of the sea to the cyclone passage is strongly influenced by a steady current when the steady current and the current due to the cyclone wind are of the same order. The steady current diminishes the sea response and reduces the speed of the southward current, and enhances the northward current speed. The intensity and the translation speed of a cyclone also influence the flow pattern significantly.

INTRODUCTION

Extra-tropical winter storms (or just cyclones for simplicity) are typical phenomena in the Yellow Sea. These cyclones are large atmospheric low pressure disturbances which strongly influence the current field of the region. The northwesterly mean wind is a common background here for the winter period. A steady current caused by the northwesterly wind and a cyclone generated current are of the same order. This particular feature defines the difference of this case from the case of a typhoon passage: typhoon generated currents normally are much stronger than the steady current. There are only a few works devoted specifically to cyclone passages in the Yellow Sea area (Hsueh *et al.*, 1986; Oh and Kim, 1990). More attention has been paid to typhoon passages rather than to cyclones. Probably this is the reason why the boundary current behaviour near the western boundary of the Yellow Sea in winter time is still unclear. Usually cyclones come from the west and pass the area eastward. They are quite variable in their tracks, translation speed, and intensity.

So, it is not easy to simulate all the corresponding effects. High pressure (anticyclones) which also influences the character of circulation in the Yellow Sea is out of interest of the present study. We would like to estimate the importance of the following factors: i) the cyclone intensity, ii) the influence of a steady current, and iii) the cyclone track.

We use the non-linear vertically integrated two-dimensional numerical model (Subbotina, 1990; Ivanov *et al.*, 1994). This model has been successfully applied, in particular, to examining the influence of non-steady wind on the generation of ring-type eddies in the Gulf Stream region. The specific feature of the model is that it takes two components of wind stress into account: steady component which forces the steady current in the sea and non-steady component caused by the cyclone passage, which generates time-varying currents. The latter could be described by the Gaussian function.

MODEL DESCRIPTION

The model is based on non-linear equations of motion, integrated over the depth. The water depth H is supposed to be a constant. Here, P is the

*Present Address: P.P. Shirshov Institute of Oceanography, Moscow 117851, Russia

pressure,

$$\frac{\partial u}{\partial t} + u\frac{\partial u}{\partial x} + v\frac{\partial u}{\partial y} - fv = -\frac{1}{\rho}\frac{\partial P}{\partial y} - Ku + \frac{\tau^x}{H} \qquad (1)$$

$$\frac{\partial v}{\partial t} + u\frac{\partial v}{\partial x} + v\frac{\partial v}{\partial y} + fu = -\frac{1}{\rho}\frac{\partial P}{\partial y} - Kv + \frac{\tau^y}{H} \qquad (2)$$

(u, v) are the horizontal components of the velocity with u in eastward (x) and v in northward (y) direction, f is the Coriolis parameter, $f = f_0 + \beta y$, $f_0 = 2\Omega$ sin ϕ_0, $\beta = (2\Omega/a)$ cos ϕ_0, Ω velocity of the earth rotation, ϕ_0 latitude for the β-plain approximation and a the radius of the earth. The bottom friction is linearly dependent on velocity with the coefficient K, which is taken as a constant. The the wind stress (τ^x, τ^y) is assumed to be a mass force. The equation (3) is the horizontally non-divergent continuity equation.

$$\frac{\partial u}{\partial x} + \frac{\partial v}{\partial y} = 0 . \qquad (3)$$

We take rigid-lid approximation here. After introducing the stream function:

$$u = -\frac{\partial \psi}{\partial y}, \quad v = \frac{\partial \psi}{\partial x}, \qquad (4)$$

and non-dimensionalizing the equations (1)-(3) (Veronis, 1966), we will get the vorticity and Poisson equations:

$$\frac{\partial \zeta}{\partial t} + RJ(\psi, \zeta) + \frac{\partial \psi}{\partial x} = -\varepsilon\zeta + rot_z \tau ; \qquad (5)$$

$$\zeta = \Delta\psi \qquad (6)$$

where Jakobian $J(\psi, \zeta) = \frac{\partial \psi}{\partial x}\frac{\partial \zeta}{\partial y} - \frac{\partial \psi}{\partial y}\frac{\partial \zeta}{\partial x}$; and

model parameters: $R = \dfrac{W_0}{\beta^2 L^3 H}$ is the non-linear parameter and $\varepsilon = \dfrac{K}{\beta L}$ is the bottom friction parameter. Here, W_0 is wind stress magnitude, and L is the horizontal length scale. We use the following values of the physical parameters:

$$\phi_0 = 35°, \qquad\qquad \Omega = 0.73 \times 10^{-4}\ s^{-1},$$
$$a = 6.4 \times 10^8\ cm, \qquad \beta = 1.98 \times 10^{-13}\ cm^{-1}\ s^{-1},$$
$$H = 4 \times 10^3\ cm, \qquad L_x = 1.26 \times 10^8\ cm, \qquad (7)$$
$$L_y = 2 \times 10^8\ cm, \qquad L = 10^8\ cm,$$
$$W_0 = 1\ cm^2\ s^{-2}, \qquad K = 0.4 \times 10^{-5}\ s^{-1}.$$

The sea is supposed to be a quasi-closed domain. The free-slip boundary condition is applied at the coast along the boundaries

$$\psi = 0 . \qquad (8)$$

Numerical integration is executed for the equations (5) and (6) with the boundary conditions (8) for the grid with the space interval 20 km (x) and 25 km (y), and time step 12 hours. We use the central difference scheme for numerical computations providing the second order of accuracy (Roach, 1976). The wind stress could be presented as it was mentioned above as a sum of steady component and cyclone component. The steady component, which is constant in time, generates a steady current system.

The cyclone stream function is presented by the Gaussian function:

$$\phi = Be^{-r^2/\sigma^2}, \qquad (9)$$

where $r^2 = (x - x_0 - U_A t)^2 + (y - y_0 - V_A t)^2$, and (x_0, y_0) are the coordinates of the cyclone center at the initial moment $t = t_0$, (U_A, V_A) are the components of the cyclone translation velocity. The cyclone parameters remain constant. The effective radius corresponds to one half of the cyclone radius. The tangential component of the wind velocity is:

$$U = \frac{\partial \phi}{\partial r} = -2B\frac{r}{\sigma^2}e^{-r^2/\sigma^2} \qquad (10)$$

From the expressions for the maximum wind speed in the cyclone

$$|U|_{max} = \left(\frac{\partial \phi}{\partial r}\right)\Big|_{r=r_1} = \left(\frac{\partial \phi}{\partial r}\right)_{max} \text{ and } \frac{\partial^2 \phi}{\partial r^2} = 0 . \qquad (11)$$

We can determine the radius of the maximum wind r_1 and the coefficient B using (9), (10) and (11). They are $r_1 = \sigma/\sqrt{2}$, $B = \sigma|U|_{max}\sqrt{e/2}$, and then the cyclone stream function becomes

$$\phi = \sigma|U|_{max}\sqrt{\frac{e}{2}}e^{-r^2/\sigma^2} \qquad (12)$$

Assume that the wind stress is a linear function of the cyclone speed:

$$\tau = CU, \ W_{max} = C \, |U|_{max}$$

where the friction coefficient $C = 10^{-3}$ cm/s. Then, the wind stress can be expressed by using W_{max}

$$\tau = -2\sigma W_{max} \frac{r}{\sigma^2} \sqrt{\frac{e}{2}} \, e^{-r^2/\sigma^2}. \tag{13}$$

We use the following expression for the wind stress curl:

$$rot_z \tau = \frac{W_{max}}{W_0} \left(\frac{L}{\sigma}\right) \left(1 - \frac{r^2}{\sigma^2}\right) e^{-r^2/\sigma^2}. \tag{14}$$

Cyclones come from the outside of the western boundary, China, and propagate eastward. That means that there is only the zonal component of the translation velocity and we use the term 'translation speed' in the following text. We take two effective radii (1000 km and 1500 km) here, with different strength, initial conditions and cyclone tracks (Table 1). The magnitudes of the effective radii are the typical scales of winter cyclone of the study area.

NUMERICAL EXPERIMENTS

Several numerical experiments have been provided to study the peculiarities of the currents in the Yellow Sea during cyclones passages. We run the model with a steady wind until the sea gets a steady current field, then run the model continuously with a translating cyclone. For each experiment, effective cyclone radius, zonal translation speed, cyclone tract, and wind speed applied are listed in Table 1.

Experiment 1: No steady wind case

The cyclone moves along the central latitude of the domain. We use zero current velocities as initial conditions. In the further text the term 'cyclone' means 'the center of the cyclone'.

Before the center comes to the region, the clockwise circulation is prevailed (Fig. 1a), and a northward western boundary current of about 4 cm/s is formed. This is because the cyclone starts influencing the current field even before the cyclone entered the sea. After the cyclone leaves the domain, the counterclockwise circulation becomes dominant (Fig. 1b, c): the southward current near the western boundary amplifies from 17 cm/s to 62 cm/s. Such a southward current retains for 6 days. On the fifth day a new clockwise circulation forms nearby the east side of the area (Fig. 1d) and pushes the cyclonic circulation towards the western boundary (Fig. 1e, f). Current speed diminishes and the circulation gradually weakens (Fig. 1g, h). During the current evolution we can see the westward moving waves with the phase speed 60 cm/s (Fig. 1d, e, f), in good agreement with the phase speed of the second mode of Rossby waves in a closed basin, which satisfy the following dispersion relation (Krauss, 1973).

$$\omega = \frac{\beta}{2\sqrt{(\frac{n\pi}{L_x})^2 + (\frac{m\pi}{L_y})^2}},$$

mode number   n and m = 1, 2, 3, $\cdots$ (15)

where ω is the wave frequency and the corresponding wave number $k = \beta/2\omega$. The speed for each mode is

Table 1. Cyclone and steady wind parameters used in the numerical experiments. (N: experiment number, σ: effective cyclone radius, U_A: zonal translation speed, Y_0: zonal cyclone track, U_{max}: maximum wind speed in the cyclone, U: speed of steady wind)

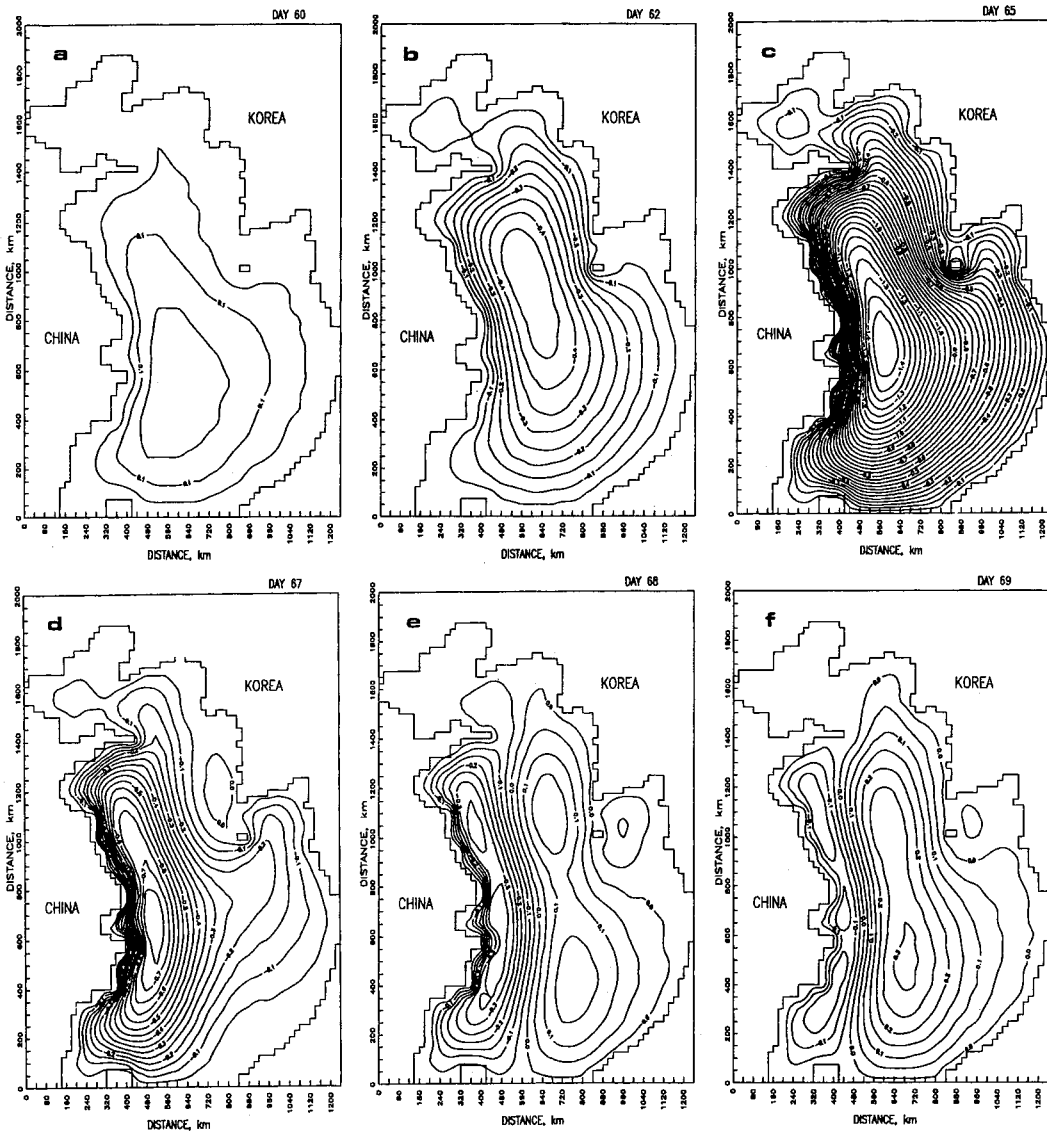| N	Cyclone				Steady wind	
	σ(km)	U_A(m/s)	Y_0	U_{max}(m/s)	U(m/s)	Wind Direction
1	1500	6	0.5 L_y	40	–	–
2	1500	6	0.5 L_y	40	10	NW
3	1500	6	0.5 L_y	60	10	NW
4	1500	6	0.5 L_y	60	5	NW
5	1500	6	0.5 L_y	40	10	SE
6	1500	6	0.01 L_y	40	–	–
7	1500	6	0.9 L_y	40	–	–
8	1500	6	0.2 L_y	40	–	–
9	1000	7.6	0.9 L_y	20	20	NW
10	1000	3.6	0.9 L_y	20	10	NW

Fig. 1. Streamlines in Experiment 1: $\sigma = 1500$ km, $U_A = 6$ m/s, maximum wind speed $U_{max} = 40$ m/s, no steady wind. The time is counted from the start of calculations. The cyclone track is in the middle of the domain, 0.5 L_y. The arrival time of the cyclone is the 59th day. (a:60th day; b:62nd day; c:65th day; d:67th day; e:68th day; f:69th day; g:70th day; h:72nd day).

listed in Table 2.

A weak northward current arises with the maximum current speed of 10 cm/s. Thus, the current near the western boundary varies in time forming at first northward current, then a southward current, and then once again a northward current. The first formation of the northward current is induced by the frontal part of the cyclone, and then the southward current is formed by the rear side of the cyclone. The next northward current generation is induced by Rossby waves.

The averaged kinetic energy distribution is shown in Fig. 2. When the cyclone comes, the kinetic energy increases and vice versa.

Experiment 2: 10 cm/s steady wind case
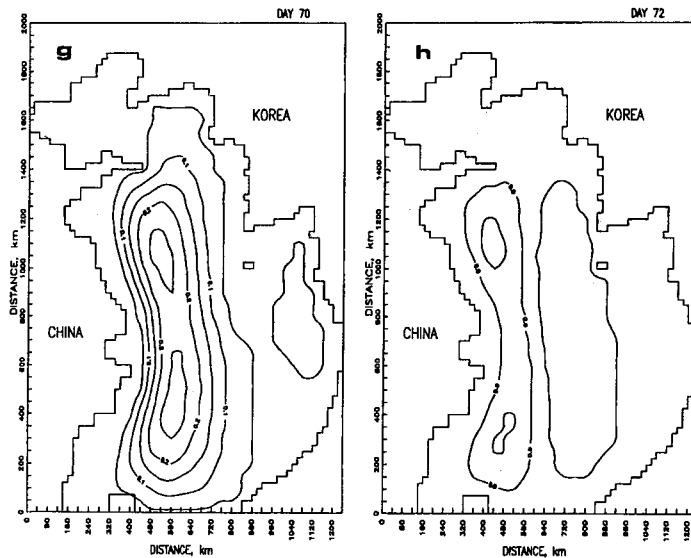
The initial condition here is the presence of a

Fig. 1. (Continued)

Table 2. Parameters of Rossby waves; ω is the wave frequency, k is the wave number, C_f is phase speed, R_0 is Rossby radius.

| mode | | $\omega \times 10^{-6}$ | $k \times 10^{-8}$ | C_f(cm/s) | R_0(km) |
n	m				
1	1	3.26	3.04	107	1000
2	1	1.82	5.44	33	577
1	2	2.44	4.06	60	774
2	2	1.63	6.07	27	518
3	1	1.24	7.98	16	394

steady current caused by the northwesterly wind of 10 m/s, which is typical for winter time (Park, 1986; Yanagi and Takahashi, 1993) (Fig. 3a).

In general, the current field variation in time is similar to that in the Experiment 1: northward current, then southward current, then once again weak northward current are formed near the western boundary. However, the northward current is stronger than in the Experiment 1, with maximum current speed up to 20 cm/s (Fig. 3b, c). After the cyclone leaves the region, the counterclockwise circulation increases significantly (Fig. 3d, e, and f), the current speed amplifies from 14 cm/s to 47 cm/s. The flow, however, is a little weaker than in the Experiment 1 and retains for shorter time (about 4 days). Afterwards, the clockwise circulation dominates in the domain and because of westward propagating Rossby waves a new northward flow of 25 cm/s appears (Fig. 3g). So we can see a similar current
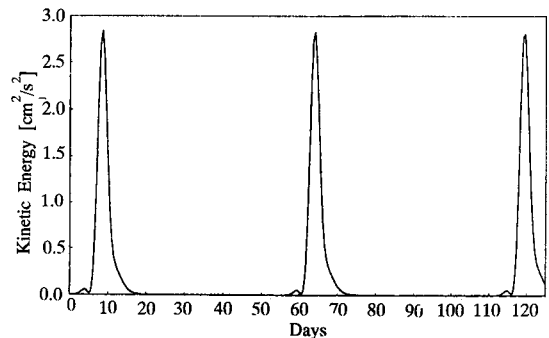

Fig. 2. Averaged kinetic energy in Experiment 1: $\sigma = 1500$ km, $U_A = 6$ m/s, maximum wind speed $U_{max} = 40$ m/s, no steady wind.

pattern (northward/southward/northward) as a result of the cyclone passage.

The averaged kinetic energy distribution differs from that observed in the Experiment 1. (Fig. 4). Comparing the energy distribution with that one observed for the sea level variations during the cyclone passage (Oh and
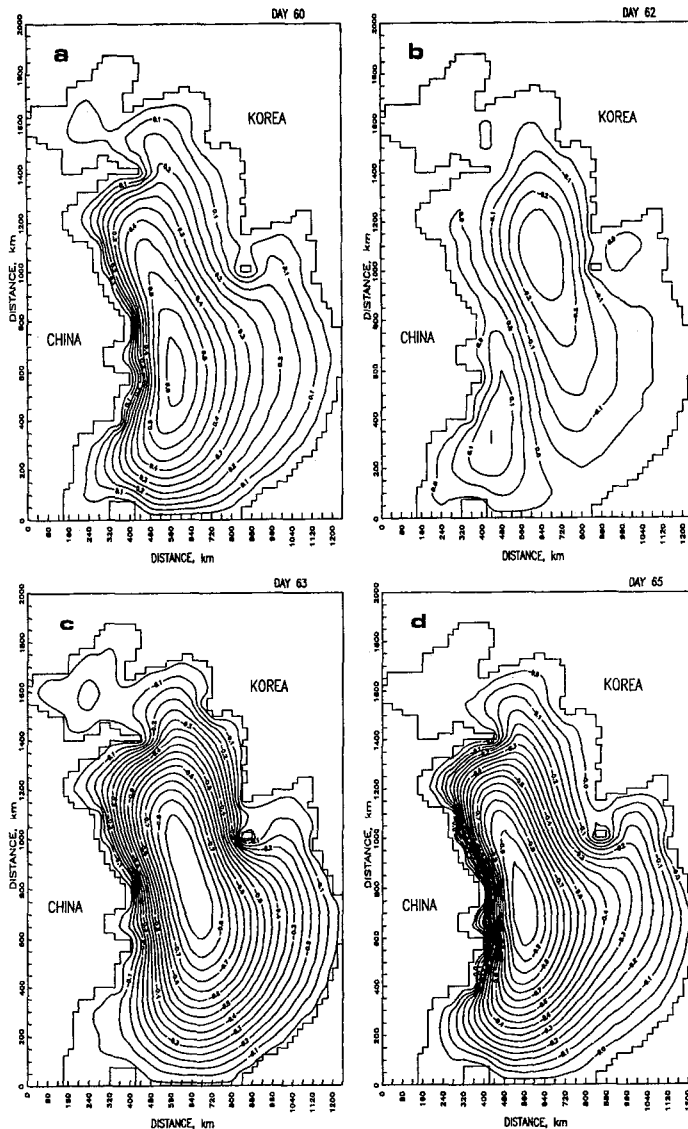
Fig. 3. Streamlines in Experiment 2: $\sigma = 1500$ km, $U_A = 6$ m/s, maximum wind speed, $U_{max} = 40$ m/s, steady northwest wind of 10 m/s. The time is counted from the start of calculations. The cyclone track is in the middle of the domain, $0.5L_y$. The arrival time of the cyclone is the 59th day. (a:60th day; b:62nd day; c:63rd day; d:65th day; e:66th day; f:67th day; g:69th day).

Kim, 1990), we see that the troughs and crests of sea levels are similar to the current variations near the western border of the present study. The steady current determines several maxima appearing in the energy fluctuations during the cyclone passage.

Experiment 3: High cyclone intensity case

The steady circulation of this experiment 3 is the same as it was in the Experiment 2. Due to the increase of the cyclone intensity with the maximum wind speed of 60 cm/s, the duration of the southward current increases up to 5 days from 4 days in the Experiment 2. The current speed here increases also from 25 cm/s to 75 cm/s. Thus, we see the essential influence of the cyclone intensity on the western current speed and duration. So the more
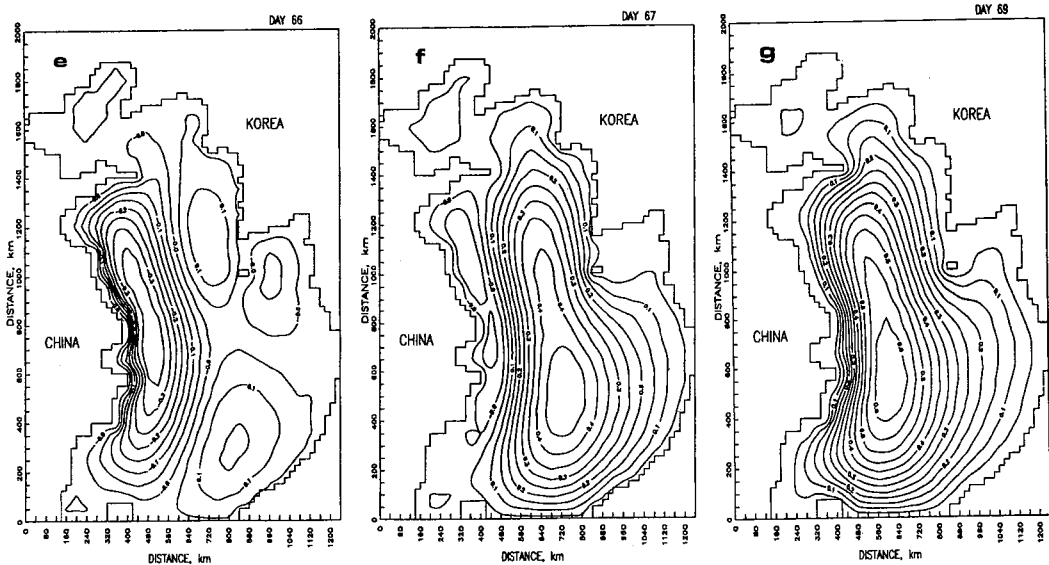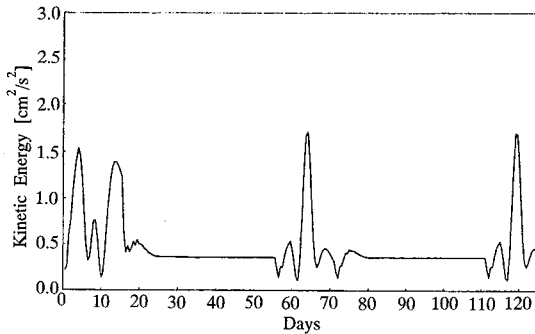
Fig. 3. (continued)

Fig. 4. Averaged kinetic energy in Experiment 2: $\sigma = 1500$ km, $U_A = 6$ m/s, maximum wind speed $U_{max} = 40$ m/s, steady northwesterly wind 10 m/s as a steady state.

intensive the cyclone is, the stronger the southward current is. The kinetic energy varies the same way as in the Experiment 1.

The main purpose of the Experiments 4 and 5 was to study how the steady circulation due to steady winds influences the response of the currents to the cyclone passage.

Experiment 4: Weak steady wind case

We consider a weak northwesterly steady wind with a speed of 5 cm/s. This wind induces a clockwise circulation in the sea, and a southward steady current near the western boundary is formed. The general pattern of the flow field is very similar to

those observed in the Experiments 2 and 3, so we do not show it here.

When a strong cyclone with the maximum wind speed of 60 cm/s approaches, the northward current of 20 cm/s near the western boundary are formed. This is somewhat smaller speed than 30 cm/s in the Experiment 3. On the other hand, the southward current at the lee side of the cyclone becomes a maximum value 90 cm/s in this experiment which was 75 cm/s in the Experiment 3. The second northward current afterwards induced by Rossby waves is of the same order as the initial one, i.e. about 30 cm/s in the Experiment 3 and about 20 cm/s in the Experiment 4.

Getting together the Experiments 2, 3, 4 and 5, we see that the amplification of the steady wind enhances the northward current and diminishes southward current near the western boundary.

Experiment 5: Southeast steady wind case

In this experiment, we consider a lower intensity cyclone ($U_{max} = 10$ cm/s) and a reversed steady wind direction, southeast wind of 10 m/s (Woodruff et al., 1987). A clockwise circulation with a steady northward current near the western boundary is formed. The approaching cyclone amplifies the northward current up to 37 cm/s (Fig. 5). After the cyclone
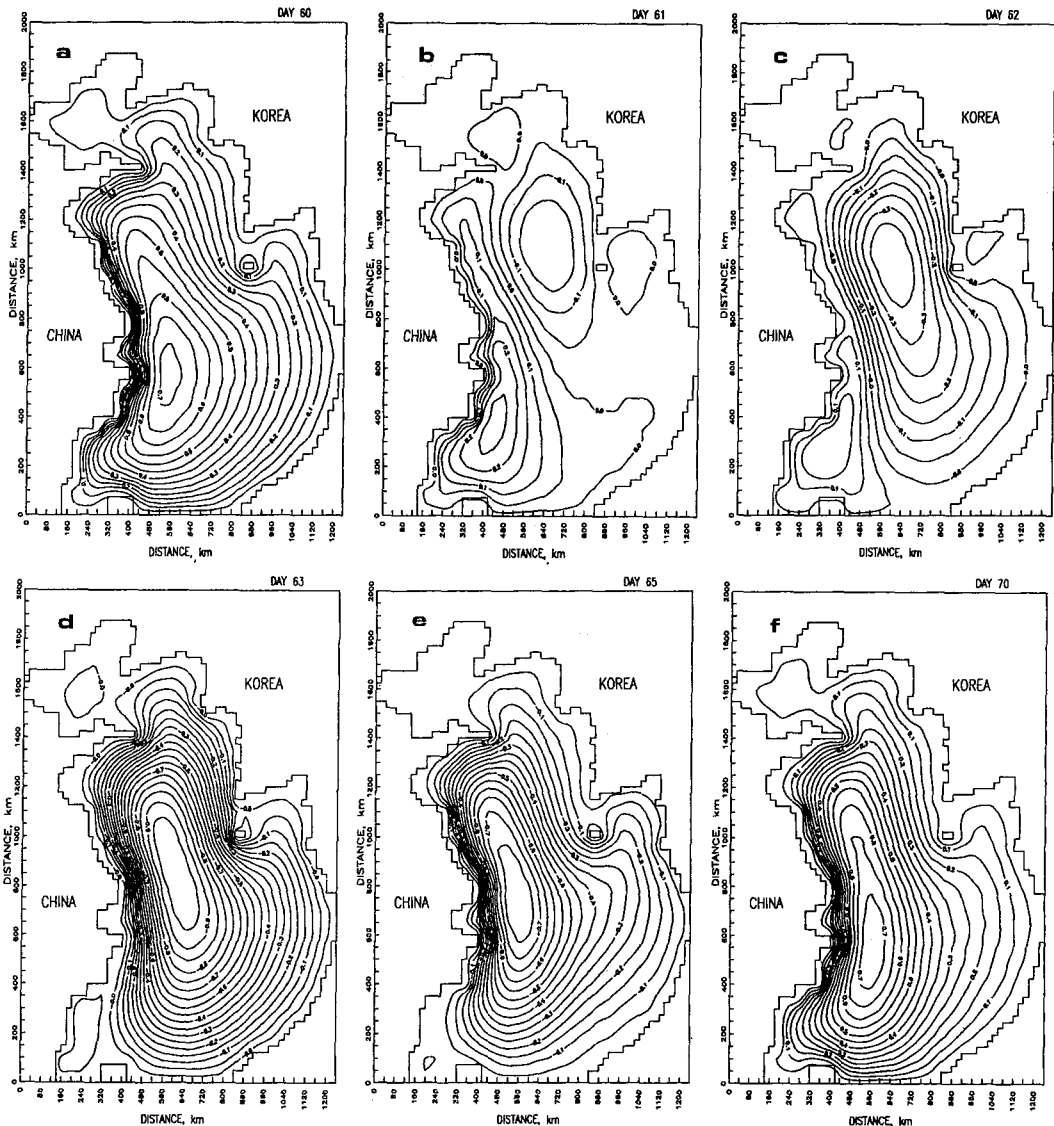
Fig. 5. Streamlines in Experiment 5:σ = 1500 km, U_A = 6 m/s, maximum wind speed U_{max} = 40 m/s, southeast steady wind of 10 m/s. The cyclone track is in the middle of the domain, 0.5L$_y$. The time is counted from the start of calculations. The arrival time of the cyclone is the 59th day. (a:60th day; b:61st day; c:62nd day; d:63rd day; e: 65th day; f:70th day).

leaves the sea area, a southward current prevails (Fig. 5b, c). This current increases from 20 cm/s up to 42 cm/s (Fig. 5d, e) and maintains for 3.5 days. Comparing with the Experiment 1, we see that the northward current caused by the steady wind, retards the southward current induced by the cyclone passage and reduces its duration (Fig. 5f).

So, in case of cyclones moving over the Yellow Sea the steady circulation is rather important. It diminishes the dynamic response of the sea to the cyclones.

Experiments 6, 7, and 8: Three different cyclone tracks

No steady wind is considered in these experiments. They have three different cyclone tracks,
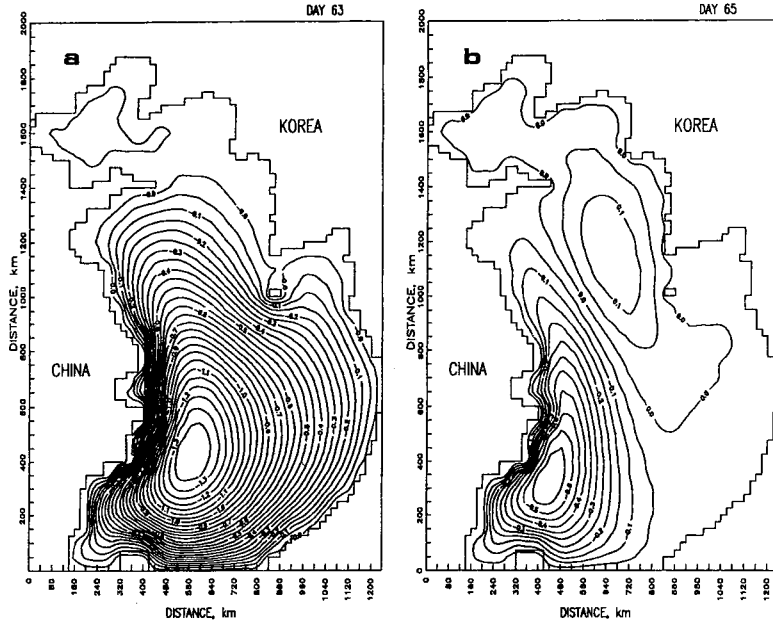
Fig. 6. Streamlines in Experiment 6: $\sigma = 1500$ km, $U_A = 6$ m/s, maximum wind speed, $U_{max} = 40$ m/s no steady wind. The cyclone track is 20 km inside the domain from the south boundary, $0.01\,L_y$. The time is counted from the start of calculations. The arrival time of the cyclone is the 58th day. (a:63rd day; b:65th day).
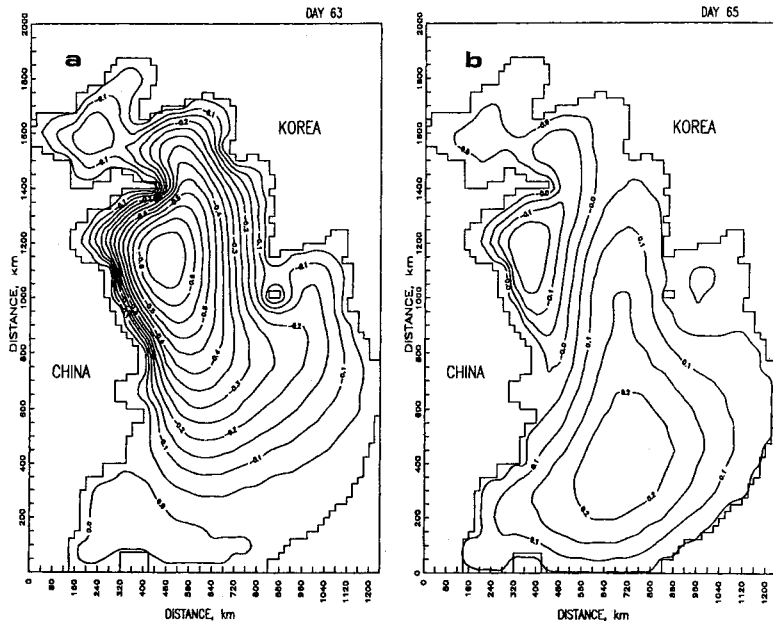

Fig. 7. Streamlines in Experiment 7: $\sigma = 1500$ km, $U_A = 6$ m/s, maximum wind speed $U_{max} = 40$ m/s, no steady state. The cyclone track is 200 km inside the domain from the north boundary, $0.9\,L_y$. The time is counted from the start of calculations. The arrival time of the cyclone is the 59th day. (a:63rd day; b:65th day).

eastward inside the domain. In the Experiment 6 the cyclone crosses the sea in 2 days, 20 km from the southern boundary (Fig. 6), and in the Experiment 7 the cyclone crosses it in a half day, 200 km from
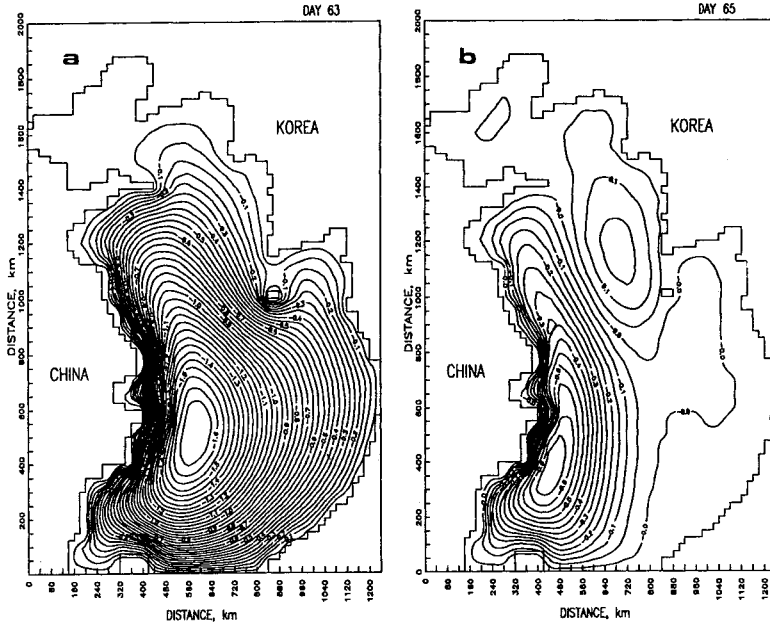
Fig. 8. Streamlines in Experiment 8: $\sigma = 1500$ km, $U_A = 6$ m/s, maximum wind speed $U_{max} = 40$ m/s, no steady wind. The cyclone track is 400 km inside the domain from the south boundary, 0.2 L_y. The time is counted from the start of calculations. The arrival time of the cyclone is the 59th day. (a:63rd day; b:65th day).

the northern boundary (Fig. 7). In the Experiment 8, the cyclone crosses the sea in 2.5 days, 400 km from the southern boundary (Fig. 8).

The cyclone track influences the time when the southward, or northward western boundary current achieves the maximum value. In the Experiment 6 the maximum speed of the southward current is larger, up to 51 cm/s (Fig. 6); the corresponding speed in the Experiment 7 is about 30 cm/s (Fig. 7). The maximum current speed has been achieved almost at the same time in both experiments. The northward currents are of the same order in all experiments: the initial northward flow is about 13 cm/s; the repeated northward current is about 5-8 cm/s. In the Experiment 8 the southward current is about 80 cm/s, much stronger than in the Experiments 6, 7 (Fig. 8). This could be explained by the longer duration of the cyclone propagation over the domain.

The point where the southward current achieves its maximum, 'maximum point' changes its position along the western boundary; it depends on the latitude of the cyclone passage. The maximum point is in 500 km (Experiment 6 and 8), 1100 km (Exper-

iment 7) from the southern boundary (Fig. 6-8). In the Experiments 1 and 2 this point was observed in 800 km from the southern boundary, where the western border has a significant cusp (Fig. 1). Thus, the 'maximum point' of the current speed depends on the cyclone track and boundary shape.

Experiments 9 and 10: Two different translation speeds

The main purpose of these experiments is to examine how a translation speed influences the response of the flow field to a cyclone. The cyclone translation speed of 6 m/s is a criterion for fast and slow moving cyclone (Price, 1981). Here, we consider two different translation speeds, 7.6 m/s and 3. 6 m/s. The cyclone track is along the latitude in 200 km from the northern boundary. The steady circulation is formed by the northwesterly wind of 10 m/s.

In the Experiment 9 after the fast cyclone leaves the sea area the counterclockwise circulation dominates. Rather weak southward current is observed in the northwestern part of the domain (Fig. 9b). This current has a maximum speed (20 cm/s) in the
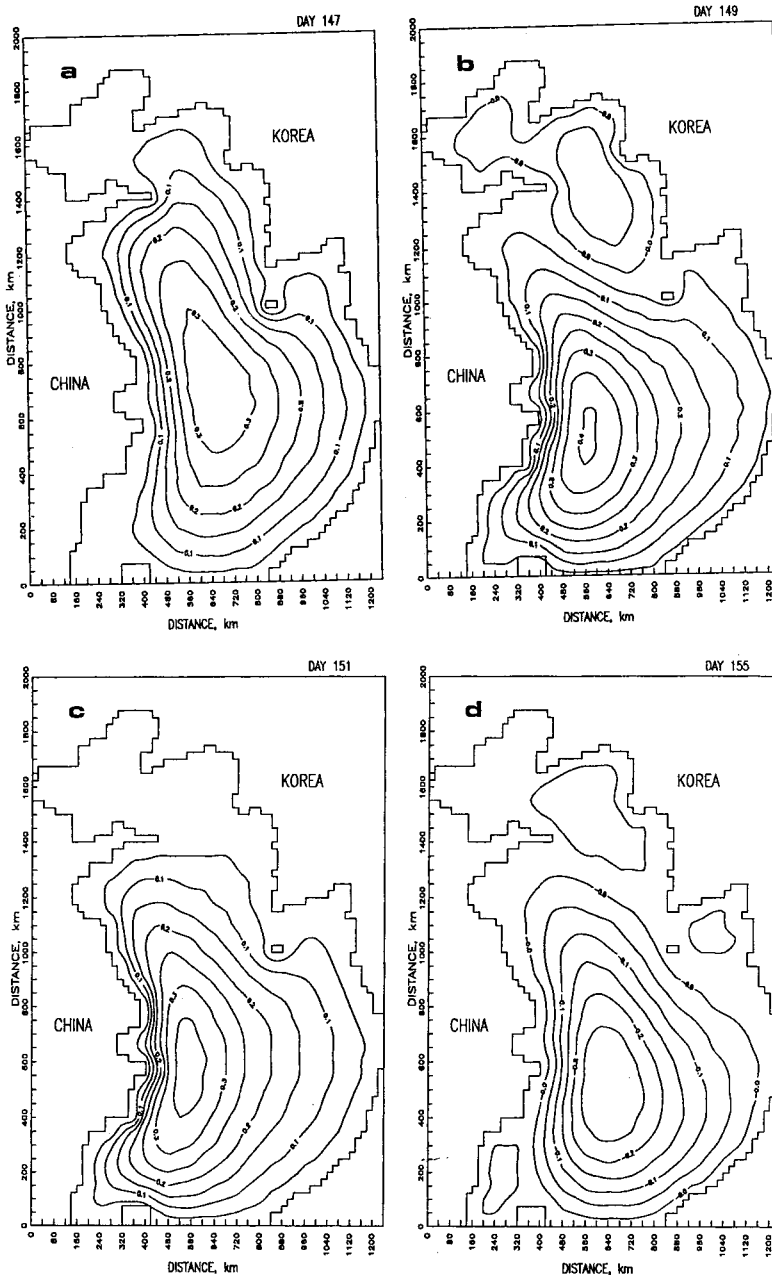
Fig. 9. Streamlines in Experiment 9: $\sigma = 1000$ km, $U_A = 7.6$ m/s, maximum wind speed $U_{max} = 20$ m/s, northwest steady wind of 10 m/s. The cyclone track is 200 km inside the domain from the northern boundary, 0.9 L_y. The time is counted from the start of calculations. The arrival time of the cyclone is the 148th day. (a:147th day; b:149th day; c:151st day; d:155th day).

next day after the cyclone leaves the sea area. The northward current in the southwestern part of the domain exists all the time while the cyclone is over the sea (Fig. 9a, b, c and d).

The translation speed in this Experiment 10 is low, 3.6 m/s, the cyclone, therefore, influences the sea area for a longer time. The maximum southward current of 20 cm/s prevails for 3 days (Fig. 10a, b).

Fig. 10. Streamlines in Experiment 10: $\sigma = 1000$ km, $U_A = 3.6$ m/s, maximum wind speed, $U_{max} = 20$ m/s, northwest steady wind of 10 m/s. The cyclone track is 200 km inside the domain from the northern boundary, 0.01 L_y. The time is counted from the start of calculations. The arrival time of the cyclone is the 122nd day. (a:122nd day; b:123rd day; c:128th day; d:135th day).

The northward current exists all the time while the cyclone influences the area (Fig. 10a, b, c and d).

SUMMARY AND CONCLUSIONS

We use a barotropic non-linear numerical model to study the response of the Yellow Sea to cyclone passage. The cyclone was approximated by the Gaussian function. We tested how the different cyc-

lone parameters: the intensity, cyclone track, translation speed, and steady current, influence the response of the currents in the Yellow Sea to the cyclone passage.

1. Before a cyclone comes into the sea area there is a slight increase of a northward current near the western boundary of the sea, which shows a good agreement with actual observations of sea levels. Then, a southward current is induced by the cyclone at its rear side. After that a new northward current is generated once again, by the westward propagating Rossby waves, which are induced by the cyclone passage.

2. Steady currents modify the dynamic response of the sea to a cyclone. It reduces the speed of the southward current, and enhances the northward current.

3. Strong wind in a cyclone amplifies southward and northward currents, as well as the time of the southward current retaining.

4. When a cyclone passes over the northern part of the domain, it induces northward current in the southern part of the sea with significant clockwise circulation. This current exists all the time during the cyclone passage. The cyclone induces also a southward current in the northern part of the sea. The strength of the current and its existence time depend on the cyclone translation speed.

5. In case of a fast cyclone with a larger translation speed than 6 m/s, a southward current appears after the cyclone leaves the domain; and in case of a slow cyclone with less speed than 6 m/s a southward current arises earlier, i.e., while the cyclone stays over the domain. The translation speed influences the time of existence of the southward current.

ACKNOWLEDGEMENTS

REFERENCES

Hsueh, Y., R. D. Romea, and P.W. E. Witt. 1986. Wintertime winds and coastal sea-level fluctuations in the north East China Sea. Part II: Numerical model. *J. Phys. Oceanogr.*, **16**: 241-261.

Ivanov, Yu. A., A. G. Novitskiy, and M. M. Subbotina. 1994. Nonstationary barotropic model of the interaction of large scale ocean gyres. (in Russian), *Transactions (Doklady) Russian Academy of Sciences*, **334**: 103-105.

Krauss, W. 1973. *Methods and Results of Theoretical Oceanography. Vol. 1. Dynamics of the Homogeneous and Quasihomogeneous Ocean.* Gebruder Borntraeger. Berlin, 302 pp.

Oh, I. S. and S. I. Kim. 1990. Numerical simulations of the storm surges in the seas around Korea. *J. Oceanol. Soc. of Korea*, **25**: 161-181.

Park, Y. H. 1986. A simple theoretical model for the upwind flow in the southern Yellow Sea. *J. Oceanol. Soc. of Korea*, **21**: 203-210.

Price, J. F. 1981. Upper ocean response to a hurricane. *J. Phys. Oceanogr.*, **11**: 153-175.

Roach, P. J. 1976. *Computational Fluid Dynamics.* Hermosa Publ., New Mexico, 446 pp.

Subbotina, M. M. 1990. The response of a barotropic ocean to a nonstationary harmonic wind forcing. *Oceanology*, **30**: 529-533.

Veronis, G. 1966. Wind-driven ocean circulation, Part II, Numerical solutions of the nonlinear problem. *Deep Sea Res.*, **13**: 31-57.

Woodruff, S. D., R. J. Slutz, R. L. Jenne, and P. M. Steurer. 1987. A comprehensive ocean-atmosphere data set. *Bull. Amer. Meteorol. Soc.*, **68**: 1239-1250.

Yanagi, T. and S. Takahashi. 1993. Seasonal variation of circulations in the East China Sea and Yellow Sea. *J. Oceanogr.* **49**: 503-520.